2.6 DIAGNOSTIC BOUNDARY LAYER HEIGHT FOR CLOUD-TOPPED BOUNDARY LAYERS IN A MESOSCALE MODEL

Daniel P. Eleuterio[1], Qing Wang[1*], and Konstantinos Rados[1]
[1]Naval Postgraduate School, Monterey, CA

1. INTRODUCTION

The depth of the atmospheric boundary layer, or boundary layer height (BLH), results from a balance between the large-scale subsidence and boundary layer entrainment depicted in Eq.(1),

$$\frac{dh}{dt} = w_e - w_s \qquad (1)$$

where h is the boundary layer height, w_e is the entrainment velocity, and w_s is the large-scale subsidence velocity. In some one-dimensional mixed layer models (e.g., Lilly 1968, Nicholls 1984), BLH is directly predicted through Eq (1), while in turbulence closure models, BLH can be diagnosed through the predicted boundary layer thermodynamic or turbulence properties. In models with high vertical resolution, diagnosing boundary layer height is straightforward, while problems may arise in a coarse-resolution model such as a mesoscale model. Thus, one needs to identify the optimal method that can be used to diagnose BLH for mesoscale model application.

In this study, we focus on the stratocumulus-topped marine boundary layers (STBL). We will first examine the observed boundary layer height and the inversion structure using measurements from a research aircraft. The results will be then used to compare with those simulated using the Naval Research Laboratory's Coupled Ocean-Atmosphere Mesoscale Prediction System (COAMPS™). Discrepancies in BLH between the model and observations may have two causes: one is the inadequate prediction of boundary layer properties in the model; the other is inappropriate diagnosis of the BLH from the modeled boundary layer properties. This study will focus on improvements to the latter.

2. OBSERVATIONS FROM DECS

Aircraft, cloud radar, radiometer and rawinsonde observations were collected along the Central California coast near Monterey Bay, California during the Dynamics and Evolution of Coastal Stratus (DECS) field study from June 13 to July 22, 1999. Twenty daytime research flights using the NPS/CIRPAS Twin Otter were made to measure MABL turbulence, thermodynamics, and cloud microphysics. The instrumentation, calibration, and data processing of the turbulence data are described in Kalogiros and Wang (2002). Figure 1

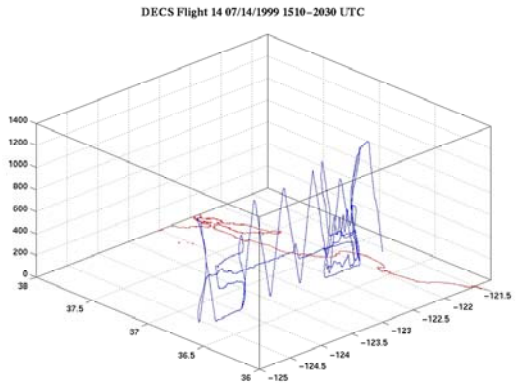

Figure 1. A typical three-dimensional flight track during DECS. Flights included multiple sounding legs through the full extent of the boundary layer, "porpoise" or sawtooth soundings providing multiple measurements across the inversion, and level leg "stacks" of constant heading and altitude for multiple levels below, within, and above the cloud layer.

depicts typical 3-D flight pattern overlaid on the California coastline. Most of the DECS flight were designed to characterize the boundary layer evolution from the coast, it thus had multiple soundings along a certain latitude and stacks of level legs for mean and

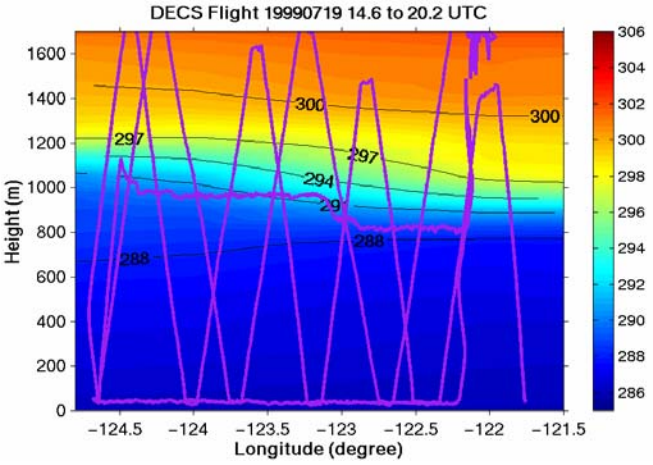

Figure 2. An example of the observed boundary layer evolution away from the coast during DECS. The contour shows the potential temperature. Solid lines denote the aircraft measurement pattern.

* *Corresponding author address:* Dr. Qing Wang, Naval Postgraduate School, Dept. of Meteorology, Monterey, CA 93940. e-mail: qwang@nps.navy.mil

turbulent statistics. Figure 2 shows the boundary layer evolution from a group of sawtooth soundings and level legs. The measurements were made on July 19, 1999. Figure 2 show the generally well-mixed boundary layer and the increase of boundary layer height away from the coastline. These features are typical of the coastal STCU MABL observed during DECS.

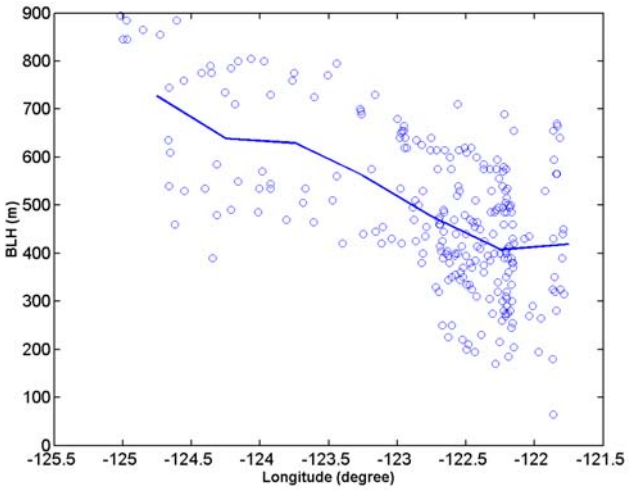

Figure 3. Variation of boundary layer height as a function of longitude. Only measurements west of Monterey Bay (between 36.5 and 37 degree latitude) are included in this dataset.

A total of 445 vertical profiles were selected from the 20 DECS flight, from which boundary layer height, inversion depth, and the jumps across the inversion in potential temperature and specific humidity were obtained. Figure 3 shows a composite of BLH variation away from the coast under typical subtropical high-pressure system (two flights were excluded because of different synoptic forcing). The increase of BLH with longitude is readily seen in this figure, where the BLH increased by about 300 m in nearly 300 km. The thickness of the inversion immediately above the boundary layer top varies significantly. Figure 4 shows the histograms of the inversion thickness and potential temperature jump across the inversion. We found that in 30% of the soundings the thickness of the inversion is less than 20 m and 70% of the soundings has an inversion of less than 100 m thick (Figure 4a). Since a mesoscale model generally has a vertical resolution of 100 m or less at the top of the boundary layer, representing the entrainment process in the mesoscale model would be challenging. In Figure 4b, we find that jump in θ across the inversion base is distributed nearly symmetrically. It has a mean of 7.5 K and a standard deviation of 3 K.

3. MESOSCALE SIMULATIONS OF THE STCU OBSERVED IN DECS

COAMPS^{TM} simulations of the marine boundary layer were made for the entire DECS period and were compared to the observations from DECS. The

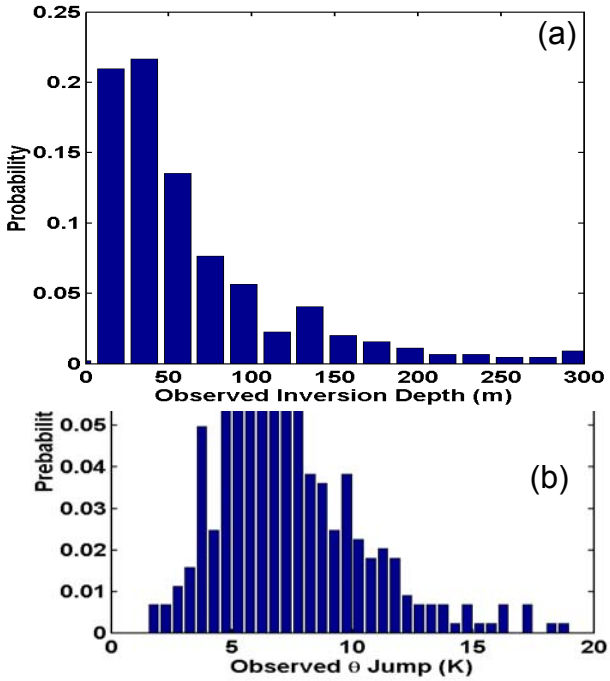

Figure 4. Probability distributions of the (a) inversion depth above the boundary layer top, and (b) the jump in potential temperature across the inversion.

simulated MABL were found to generally match the climatology for the California coastal region with a downward sloping inversion at MABL top towards the east and north, intersecting the coastal mountains, and increasing again in height over land. Additionally there was significant mesoscale variability within 100 km of the coast due to interaction between the mean flow and the coastal terrain.

Qualitatively, COAMPS^{TM} reproduced the mesoscale variability and synoptic and diurnal evolution of the MABL quite well. However, it was noted that in cloudy cases in particular COAMPS^{TM} frequently produced a low bias in boundary layer height and a high bias in liquid water path (LWP). Furthermore the model was generally 1-2 hours late to dissipate fog and stratus over land and frequently produced surface fog instead of the observed stratus over water within 100 km off the coast. It was found that, in addition to a general low bias in BLHT of 100 m, under certain cases the BLHT was significantly lower than the observations by several hundred meters. These trends were investigated in more detail by comparing all available slant path soundings from DECS to the corresponding COAMPS^{TM} forecasts. In this study, we will focus on the diagnostic boundary layer height.

4. DIAGNOSING THE BOUNDARY LAYER HEIGHT

The boundary layer height in COAMPS^{TM} is diagnosed based on Richardson number. It first identifies the lowest level at which the bulk Richardson number exceeds a critical value, which is set as 0.5 in

the model, and then interpolates linearly between this level and the level below to calculate the height where the Richardson number exceeds the critical value. Thus, the diagnosed boundary layer height may not be at the grid level. The theoretical basis for this is that when the Richardson Number is greater than a critical value, generally taken to be 0.25, the flow becomes non-turbulent. When the equations are cast in a finite difference form, the appropriate critical value at discrete grid levels becomes less certain. By examining a variety of boundary layer and inversion conditions and comparing modeled structure to aircraft sounding data, we refine the diagnostic method to ensure accurate representation of the model boundary layer.

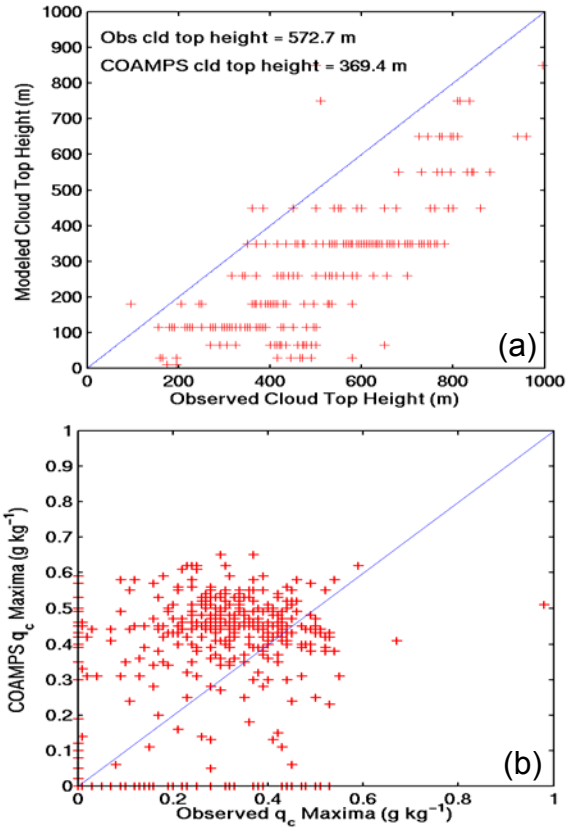

Figure 5. Comparison between the COAMPS™ simulated and observed (a) boundary layer height, and (b) maximum cloud liquid water.

Figure 5 shows the comparison between COAMPS™ simulated and DECS observed boundary layer height and maximum in-cloud liquid water. We found the COAMPS™ consistently underestimates the BLH by about 200 m and overestimates the maximum cloud liquid water (0.35 g kg^{-1} vs. 0.27 g kg^{-1} mean values).

The method for diagnosing boundary layer height is investigated here since it is a possible reason for the consistent underestimates of the BLH shown in Figure 5. To find a better diagnostic indicator for boundary layer height, one needs a variable independent from the bulk Richardson number. For the stratocumulus-topped boundary layer, a natural choice is the cloud top. Since liquid water generally increases with height in stratiform marine clouds and rapidly drops to zero just above the maximum value (Albrecht et al. 1988), the cloud top can be considered as the height where cloud liquid water reaches a maximum. Figure 6 shows a comparison between the height of maximum liquid water content (cloud top height) and the boundary layer height from all DECS soundings made by the Twin Otter. Here the boundary layer height was selected manually from the height at which the largest gradients in total water mixing ratio and liquid water potential temperature are co-located.

As can be seen in Figure 6, the observed cloud top and the height of the strongest temperature and moisture gradients are nearly the same with a mean difference of about 12 m. Thus the observations show that the cloud top height is a good indicator for boundary layer height in this regime. Using cloud top height as a measure, boundary layer height was diagnosed using three different criteria: the Richardson number, the

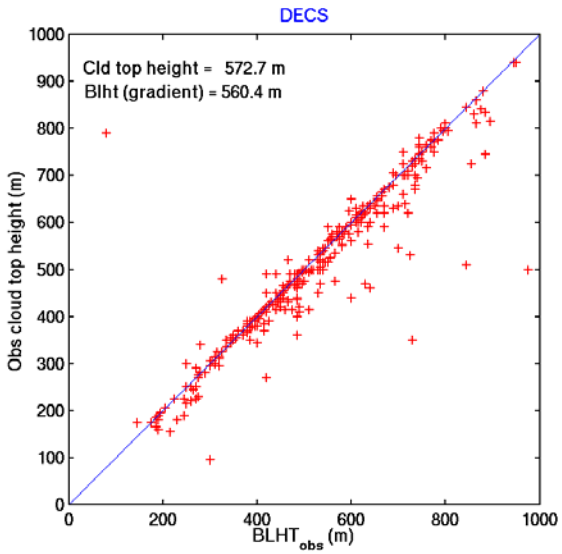

Figure 6. Comparison of the observed cloud top height and inversion height based on the vertical gradient of liquid virtual potential temperature for 445 slant-path aircraft soundings.

liquid potential temperature vertical gradient ($d\theta_l/dz$), and the water vapor mixing ratio vertical gradient (dq_t/dz). The latter two criteria are based on the fact that these gradients typically are largest at the boundary layer top in the marine CTBL and are referred to as the inversion strength methods. The diagnostic boundary layers in comparison with the modeled cloud top height are shown in Figure 7. Since no interpolation was made between two grid levels in the inversion strength method, the diagnostic BLHs are always on the grid level. The results in Figures 7b and 7c show that the

$d\theta_l/dz$ based inversion strength method gave much better results than the Richardson number or dq_t/dz based methods. It is also seen in Figure 7 that the inversion strength methods also eliminates the results in the lower right corner of Figure 7a when the diagnostic boundary layer height is much smaller than the cloud top height. Those data points were due to the presence of a stable layer close to the surface in case of boundary layer decoupling or in the presence of a surface based inversion occurring mostly over cold sea surface. Thus, using the inversion strength method would eliminate the false boundary layer definition when sub-cloud stable layers are present. These methods, however, require empirical thresholds for the gradients. The results shown in Figure 7b and 7c used a critical value of 0.02 K m^{-1} for θ_l gradient and an empirical value of -0.0065 g kg^{-1} m^{-1} for the q_t gradient. These values were empirically derived for this dataset and would likely be sensitive to the strength of the subsidence and the boundary layer dynamics.

5. SUMMARY AND CONCLUSIONS

Vertical profiles of the stratocumulus-topped marine boundary layers have been obtained by a research airplane made and analyzed to examine the boundary layer height and the inversion structure off the coast of Monterey CA. This dataset is also used to evaluate the boundary layer height and prediction of cloud water in COAMPS™. By testing different schemes of diagnosing boundary layer height, we found that the cloud top height, or BLH diagnosed using the vertical gradient of liquid water potential temperature ($d\theta_l/dz$) performed better than the Richardson number method or the total water gradient method for the cloud topped boundary layer. Note the inversion strength methods would not work in clear boundary layers or when there is a weak temperature gradient at the boundary layer top. Since the Richardson number-based boundary layer height generally works well for the clear boundary layer (not shown), we used a hybrid approach that diagnoses the BLH using the cloud top or inversion strength method for cloudy boundary layer and the Richardson number method for the clear boundary layers.

It should be noted that improvement in diagnosing boundary layer height is only part of the solution to improve boundary layer prediction. Full improvement of the boundary layer properties relies on improvement of model physics. One of the model physics is the entrainment parameterization, which is done implicitly in the 1.5 order turbulence closure model in COAMPS™. The tendency of underestimating BLH and overestimating cloud liquid water shown in this paper seem to be consistent with inefficient entrainment mixing at the boundary layer top in current COAMPS™. Efforts are underway to incorporate explicit entrainment parameterization (Grenier and Bretherton, 2001) in COAMPS™ to enhance entrainment mixing at the boundary layer top.

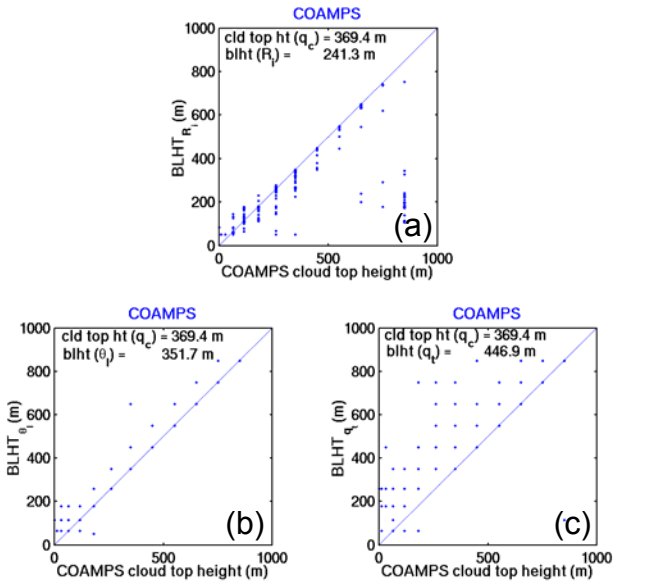

Figure 7. Comparison of the boundary layer height diagnosed based on (a) the bulk Richardson number; (b) BLHs based on vertical gradient of liquid potential temperature and c) BLHs based on total water mixing ratio. Note the cluster of misdiagnosed BLHT to the lower right in (a).

6. ACKNOWLEDGEMENTS

The authors acknowledge John Kalogiros, Haf Jonsson, Dick Lind, and Bob Creasey for their efforts in DECS measurements and assistance in the surface met observations co-located with our flight data. This research was supported by National Science Foundation grants and ATM-9900496 and Office of Naval Research Award N0001403WR20193.

7. REFERENCES

Albrecht, B. A., D. A. Randall, and S. Nicholls, 1988: Observations of marine stratocumulus during FIRE. *Bull. Amer. Met. Soc.*, **69**, 618-626.

Chen, S. and Coauthors, 2003: COAMPS™ Version 3 Model Description – General Theory and Equations. NRL Publication NRL/PU/7500—03-448, May 2003, 145 pages.

Grenier, H. and C. S. Bretherton, 2001: A moist PBL parameterization for large-scale models and its application to subtropical cloud-topped marine boundary layers. *Mon. Wea. Rev.*, **129** (3),357-377.

Kalogiros J. A. and Q. Wang, 2002: Calibration of a radome-differential GPS system on a twin otter research aircraft for turbulence measurements. *J. Atmos. Ocean Tech.* **19**: 159-171.

Lilly, D. K., 1968: Models of cloud-topped mixed layers under a strong inversion. *Quart. J. Roy. Meteor. Soc.*, **94**, 292-309